LAWRENCE
LIVERMORE
NATIONAL
LABORATORY

UCRL-JRNL-220433

Scaling laws for collisionless laser-plasma interactions of relevance for laboratory astrophysics

D. D. Ryutov, B. A. Remington

April 6, 2006

Astrophysics and Space Science

Disclaimer

Scaling laws for collisionless laser–plasma interactions of relevance for laboratory astrophysics

D.D. Ryutov, B.A. Remington

Lawrence Livermore National Laboratory, Livermore, CA 94551, USA

Abstract

Scaling laws for interaction of ultra-intense laser beams with a collisionless plasmas are discussed. Special attention is paid to the problem of the collective ion acceleration. Symmetry arguments in application to the generation of the poloidal magnetic field are presented. A heuristic model for evaluating the magnetic field strength is proposed.

1. Introduction

Interaction of ultra-intense laser radiation with a plasma is of significant potential interest for laboratory astrophysics. In particular, it opens up a possibility of creating a platform for studying such effects as generation of dynamically-significant magnetic fields [1,2], development of various collective instabilities, e.g., the filamentation instability [3,4], particle acceleration via collective effects [5-7], and dynamics of relativistic plasmas [8, 9].

At these very high intensities, the Coulomb collisions often become sub-dominant, and the plasma behavior can be reasonably well described in the collisionless approximation. Recently, first steps have been made in developing scaling relations that would govern such situations [10-13].

The amplitude E_0 of the incident wave defines the so called dimensionless vector potential,

$$a_0 \equiv \frac{eE_0}{m\omega c}. \qquad (1)$$

Here we use the CGS-Gaussian system of units, with e and m being the charge and the mass of the positron, c being the speed of light, and E_0 and ω being the electric field amplitude and the wave frequency. The parameter a_0 is the ratio of the electron quiver momentum normalized to mc. In the case a_0>1 the oscillating electrons are relativistic, with $\gamma \sim a_0$. An intensity $I \equiv cE_0^2/8\pi$ is related to a_0 by

$$I(W/cm^2) \approx a_0^2 \frac{1.8\times 10^{18}}{\left[\lambda(\mu m)\right]^2}. \qquad (2)$$

For completeness, we also present the amplitude of the oscillating magnetic field in vacuum in terms of a_0:

$$B_0(MG) = a_0 \frac{105}{\lambda(\mu m)}. \qquad (3)$$

Note that, for a typical wavelength of $\lambda \sim 1$ μm and a mildly relativistic incident wave ($a_0 \sim 1$), this oscillating field is already quite high, ~ 100MG.

One of the most efficient applications of the scaling laws is their use for testing the applicability limits of various physical models. The main assumption of Refs. [12, 13], in addition to the absence of collisions, is that the initial plasma temperature is

negligible compared to the energies that electrons and ions (if the ion dynamics is essential) acquire early in the laser pulse. Following this line, in Sec. 2 we consider possible experiments that would verify our scaling laws in the problem of the ion acceleration in the setting of Refs. [6, 7]. If the model is shown to be valid, then scaling arguments can be used as a predictive tool. We present an example of that, again using the problem of the ion acceleration, in Sec. 2.

The presence of scaling laws reveals continuous symmetries of the problem. Of a comparable importance in a number of cases are discrete symmetries, allowing one to make very general conclusions regarding the geometrical properties of the system. An example of using such symmetries in the problem of generation of the quasi-static poloidal magnetic field was given in Ref. [12], where the geometrical structure of such a field was established. Now, in Sec. 3, we extend the analysis of Ref. [12] to add a heuristic estimate of the magnitude of the poloidal magnetic field.

Throughout this paper we assume that the duration of the ultra-intense pulse τ is much greater than the wave period $2\pi/\omega$ (Fig. 1). The shape of the envelope function F has to remain the same throughout the scaling exercise, although normalization can vary.

2. Scaling for the ion acceleration experiment

In this section, we consider a standard setting for the experiment on the ion acceleration with a pulsed laser. The ultra-intense pulse hits the surface of a thin foil, where some blow-off-plasma already created by a pre-pulse is usually present. The incident beam generates ultra-relativistic electrons which cannot leave the system because of a quasineutrality constraint. These electrons start oscillating in an ambipolar potential well. On the rear surface, the hydrogen-containing impurities liberate hydrogen ions, which are accelerated by this ambipolar field, roughly speaking, in the normal direction to the foil. For a thin-enough foil, the fast electrons make many bounces inside the well, before they lose their energy. The ion acceleration by the ambipolar electric field is not affected by collisions. In other words, the ions can be treated as collisionless. We note that the foil in this discussion plays a passive role and is not involved in the process of the energy transfer from the oscillating electrons to the ions. In order for this to be correct, the foil has to be thin enough so as to make energy losses of "oscillating" relativistic electrons negligible. One can also note in passing that a very similar setting has been studied in great detail in the problem of ion acceleration by electrons generated in a high-current diode and injected into vacuum (e.g., [14-16]; see also survey [17] of these early studies).

The full set of the Maxwell-Vlasov equations describing collisionless plasmas, with relativistic electrons and non-relativistic ions was reduced to the dimensionless form in Refs. [12, 13]. It was shown that, under the conditions described above, the system is fully characterized by the following six parameters:

$$n,\ L,\ \tau,\ \omega,\ E_0,\ M/Z, \tag{4}$$

which are: the density at a characteristic point of the blow-off plasma; length-scale (e.g., spot size) of the incident beam and the blow-off plasma; the pulse duration τ of the main pulse; the frequency ω of the incident radiation; the maximum amplitude E_0 of the electric field of the incident wave (or, equivalently, the maximum intensity I), and the

mass-to-charge ratio for the accelerated ions. [The latter parameter may be of interest in the context of comparing the acceleration of hydrogen *vs.* deuterium.]

The dimensionless parameters that determine the scalability between any two (or more) systems are [12, 13]:

$$T \equiv \omega\tau;\ R \equiv L\omega/c;\ S \equiv \frac{4\pi n_0 ec}{E_0\omega};\ U \equiv \sqrt{\frac{ZeE_0}{M\omega c}}. \qquad (5)$$

They must be held constant in order that the dimensionless equations remain unchanged between the two systems such that the evolution of these systems is similar.

In addition to holding the dimensionless parameters (5) constant, in order that the two systems behave in a scaled fashion, the geometric similarities must also be observed, e.g., if the characteristic length-scale L of the plasma density distribution is increased by a factor of 2, so too must the focal spot radius be increased by the same factor. The geometrical characteristics of the incident radiation have to be identical between the two systems (up to the length-scale change): the polarization must remain the same, as well as the direction and the convergence of the incident beam. The shape of the temporal dependence of the laser pulse must also remain unchanged (although its duration may change). Under such conditions, any systems for which the dimensionless parameters (5) are kept the same, behave identically, up to scale transformations identified in Ref. [12, 13]. Here we discuss, at a conceptual level, the possible experimental verification of the underlying physics assumptions, of which the most important are the absence of collisions and smallness of the initial "temperature." Within these two assumptions, the similarity covers all the processes involved, in all their complexity: distribution functions, the spatio-temporal characteristics of the reflected waves, possible presence of the filamentation and other instabilities, magnetic field generation, and so on.

Any observed differences may signify that either the basic assumptions are wrong (e.g., the system is actually collisional), or the two experiments are not perfectly similar in terms of their geometry (including the irradiation geometry), or the temporal dependence of the incident radiation.

We have six input parameters (Eq. (4)) subject to four constraints S=const, R=const, T=const, and U= const (Eq. (5)). To check the validity of scaling laws, we can arbitrarily choose any two of six input parameters in the primed system, then adjust the remaining four so as to keep the dimensionless parameters (Eq. (5)) constant. Consider, for example, that we increase the ion mass by a factor of 2 (switching from hydrogen to deuterium), and increase the intensity by a factor of 4 (columns 2 and 3 in TABLE 1). Then, the rest of the input parameters would have to be changed as shown in columns 4-7 of Table 1. This ensures the constancy of the dimensionless parameters (Eq. (5)). The other parameters of the two systems (e.g., the average energy of the accelerated ions) changes according to the scalings formulated in Ref. [13]. Specifically, in our example, the average energy increases by a factor of 2, and the total number of accelerated ions also increases by a factor of 2 (columns 9, 11)

One can also reverse these arguments and, if there is a good reason to believe in the validity of the underlying assumptions, use the scalings as a predictive tool. For example, if an experimentalist is interested in generating fast protons with a laser with a frequency two times less than in the earlier successful experiment, he/she can do it in a scaled fashion, thereby being able to predict all the details of a new experiment. This is illustrated by TABLE 2 which shows that the same number of fast ions with the same

energy can be generated if the intensity is reduced by a factor of 4, and the other "input" parameters are changed according to the columns 4-6 of TABLE 2.

3. Discrete symmetries and generation of the poloidal magnetic field.

A variety of mechanisms for generation of a quasi-static magnetic field have been discussed in the past, including the thermo-electric dynamo [17] and a ponderomotive force [18]. These mechanisms easily explain the appearance of the toroidal magnetic field, as shown in Fig. 2a for a circular beam imprint. The experiments on the magnetic field generation carried out thus far have been interpreted in terms of the toroidal field [1, 19, 20], without much consideration given to the possible presence of the poloidal field. However, as was pointed out in Ref. [12], the symmetry arguments lead to the prediction that a poloidal magnetic field can also be generated, if the incident radiation is linearly polarized; a peculiar structure of the currents generating this field had been predicted. In this article, we provide a more detailed description of the geometrical structure and present a rough heuristic estimate of the poloidal field.

We consider the following model: A linearly polarized laser beam falls normally onto the plasma slab (Fig. 2b). The beam imprint is assumed to be circular, with the characteristic radius r_0 exceeding the wave-length of the incident light,

$$r_0 >> \lambda \qquad (6)$$

The plasma density varies in the z direction (normal to the slab) from zero to some constant value, which can be both lower and higher than the critical density. The intensity of the beam varies along z due to effects of absorption (we do not specify the mechanism) and varying density (including possible cut-off beyond the critical point). We assume that the intensity of the reflected wave is small (because of the absorption of the incident radiation, or because of a smoothness of the density variation in the case where the maximum density is sub-critical). We assume that the electric field of the incident wave is parallel to y.

As the system has two symmetry planes (xz and yz), the quasi-static current (which is a polar vector) normal to these planes must vanish (there is no preferential direction). Accordingly, the current pattern will look as shown in Fig. 2b. The shape of the streamlines is identical in all four quadrants, whereas the directions of the currents are shown by arrows. In principle, finer structures (but possessing the same symmetry) can also be present. The current of this form has some finite extent along the z axis. One can think of the current pattern as that of four solenoids of a finite length along the z axis, with the current direction alternating from one solenoid to another as shown in Fig. 2b. The distribution of the axial (z) magnetic field intensity in the xy plane at some depth z is shown in Fig. 2c by shading in pink (direction towards the viewer), and green (away from the viewer). In the limiting case of a small axial extent, the magnetic field structure will be that shown in Fig. 3: this would be a field of four current rings, with alternating direction of the currents. The aforementioned "canopy" of the magnetic field lines shows up, reminiscent of the field lines of a group of sunspots.

Thus far, we have been using only symmetry arguments, without discussing the mechanism of the poloidal magnetic field generation. Below, we provide some initial heuristic assessment.

In the case of a relativistic drive, the amplitude of the electron periodic excursions in the wave field is of the order of c/ω. For the focal spot size $r_0 >> \lambda$, this displacement is much less than the spot size. The presence of the radial gradient of the intensity under such circumstances creates an average force $\boldsymbol{f}$ acting on the electrons and varying over a scale $\sim r_0$; for generation of the poloidal magnetic field the x and y components of the force are important, as they can create the electron flow pattern shown in Fig. 2b. One should note that, for a non-relativistic drive, $a_0 << 1$, this force is potential (a so-called Miller force [21]). As we shall see, the potential force $\boldsymbol{f}$ cannot drive a quasi-static field, i.e., the condition of $a_0 > 1$ (Eq. (1)) is important for our model.

By averaging the electron momentum equation over the wave period and a spatial scale of a few wave-lengths, one obtains an equation for the evolution of thus averaged quantities:

$$\frac{d\langle \boldsymbol{p} \rangle}{dt} = \langle \boldsymbol{f} \rangle - e\langle \boldsymbol{E} \rangle - \frac{e}{c}\langle \mathbf{v} \rangle \times \langle \boldsymbol{B} \rangle \qquad (7)$$

Here $\langle \mathbf{v} \rangle$ represents the average velocity of the electrons, related by the equation $\langle \boldsymbol{j} \rangle = -en\langle \mathbf{v} \rangle$ to the average current density $\langle \boldsymbol{j} \rangle$. Neglecting for a while the electron inertia (the lhs) and the Hall effect (the last term in the rhs), and using the Maxwell equation $\nabla \times \langle \boldsymbol{E} \rangle = -(1/c)\partial \langle \boldsymbol{B} \rangle / \partial t$, one obtains:

$$\frac{\partial \langle \boldsymbol{B} \rangle}{\partial t} = -\frac{c}{e}\nabla \times \langle \boldsymbol{f} \rangle \qquad (8)$$

One sees that, indeed, the generation of the magnetic field requires the presence of a solenoidal component of the ponderomotive force, which is absent in the case of a non-relativistic drive. Eq. (8) also shows that, after the laser drive turns on, the magnetic field increases and reaches a steady state by the time when the drive ends (we shall see shortly that it may actually reach a saturation earlier, if the neglected Hall term comes into play).

We limit ourselves to a qualitative, order-of-magnitude estimate of the absolute value of the ponderomotive force. As it is related to the radial gradient of the intensity, it can be evaluated as

$$f \sim \gamma mc^2 / r_0. \qquad (9)$$

This estimate is valid only in relativistic domain, at $\gamma - 1 > 1$. The geometrical structure of the force is similar to the current pattern shown in Fig. 2b. In the approximation described by Eq. (8), the maximum magnetic field will be reached at the end of the pulse and will be equal to

$$\left| \langle \boldsymbol{B} \rangle \right| \sim \frac{\gamma mc^3 \tau}{er_0^2} \qquad (10)$$

This is a rough, order-of-magnitude estimate.

Let us now evaluate the possible contribution of the neglected terms. The complete version of Eq. (8) reads as:

$$\frac{\partial \langle \boldsymbol{B} \rangle}{\partial t} = -\frac{c}{e}\nabla \times \langle \boldsymbol{f} \rangle + \nabla \times \left\{ \left[\langle \mathbf{v} \rangle \times \langle \boldsymbol{B} \rangle \right] + \frac{c}{e}\langle \dot{\boldsymbol{p}} \rangle \right\} \qquad (11)$$

Noting that $\langle \dot{\boldsymbol{p}} \rangle \sim \gamma m \langle \dot{\mathbf{v}} \rangle \sim \gamma m \langle \dot{\boldsymbol{j}} \rangle / en \sim (\gamma mc / 4\pi en)\nabla \times \langle \dot{\boldsymbol{B}} \rangle$ and comparing the last term in the rhs with $\partial \langle \boldsymbol{B} \rangle / \partial t$, one finds that the inertial term can be neglected if

$$\frac{\gamma mc^2}{4\pi ne^2 r_0^2} \equiv \frac{c^2}{\omega_{pe}'^2 r_0^2} << 1, \qquad (12)$$

where ω'_{pe} is a relativistically-corrected cut-off frequency. As the wave frequency is typically comparable to the cut-off frequency, this condition is automatically satisfied provided the condition (6) holds.

Now we assess the role of the Hall term. By using the relation $\langle \mathbf{v} \rangle = -\langle \boldsymbol{j} \rangle / en = -(c/4\pi en)\nabla \times \langle \boldsymbol{B} \rangle$, one can rewrite Eq. (11) in the following way:

$$\frac{\partial \langle \boldsymbol{B} \rangle}{\partial t} = -\frac{c}{e}\nabla \times \langle \boldsymbol{f} \rangle - \frac{e}{mc}\nabla \times \frac{\langle \boldsymbol{B} \rangle \times \nabla \times \langle \boldsymbol{B} \rangle}{\omega_{pe}^2}. \qquad (13)$$

As the last term is non-linear in B, it would lead to the saturation of the magnetic field for a long-enough pulse. By balancing the forcing term, with f as in Eq. (9), and the Hall term, one finds the following rough estimate for the saturated field:

$$\frac{\left|\langle \boldsymbol{B} \rangle\right|^2}{4\pi} \sim \gamma m c^2 n. \qquad (14)$$

One can combine the estimate (10) and (14) in one heuristic relation, which covers both cases of a long and short driving pulses:

$$B = \frac{B_0 \tau}{\tau + (2\pi r_0/\lambda)(r_0/c)} \qquad (15)$$

with B_0 as in Eq. (3). Here we assumed that the incident wave has a frequency near a cut-off frequency. Not surprisingly, Eq. (15) can be presented in terms of B_0 and the scaling parameters R and T: $B = B_0/[1 + T/R^2]$, with r_0 playing the role of the length-scale.

Thus far, in the analysis of the magnetic field, we didn't take into account the ion motion. In reality, due to the quasineutrality constraint, they will experience a force comparable to f (although, generally speaking, of a different structure). This would cause the whole plasma in the focal spot to expand. The condition that the expansion is negligible during the time τ, reads as:

$$\tau < \frac{r_0}{c}\sqrt{\frac{M}{\gamma m Z}} \qquad (16)$$

If the opposite condition is valid, the zone of a high magnetic field is disassembled before the end of the pulse.

It goes without saying that the poloidal field may be generated alongside the toroidal field, which we do not discuss in this paper.

4. Discussion

In this paper we applied scaling and symmetry arguments to study two problems in the area of interaction of ultra-intense light with a plasma. The first problem is that of a collective ion acceleration by the ambipolar field where we identified a possible experimental test of the physics model based on the two key assumptions: 1) that the system can be described reasonably well as collisionless, for both fast electrons and ions; 2) that the initial thermal spread is negligibly small compared to the energies that they acquire early upon arrival of the ultra-intense pulse. We discuss possible way of experimental verification of this model by performing properly scaled experiments conducted so as to satisfy the similarity rules established in Refs. [12, 13]. What is very attractive with this approach is that, if the similarity indeed holds, there are many experimental signatures of that, starting from the spectrum and spatio-temporal behavior

of accelerated ions, through the quasi-static magnetic field evolution, and ending up with the spatio-temporal dependence of the reflected radiation. Deviations from the predictions of the scaling laws, in a carefully performed experiment, would mean the violation of the initial basic assumptions and would allow one to circumscribe a parameter domain in which the model is applicable. On the other hand, if the validity of the model is established, one can use the scaling laws as a predictive tool.

In the second part of the paper, based on the symmetry consideration, we establish a spatial structure of the poloidal magnetic field which may be generated alongside the toroidal field. For a linearly-polarized wave, the axial component of the field changes sign from one quadrant to the other. This is a signature that can be used if an experimental attempt to detect this field is made.

Acknowledgment

The authors are grateful to B.I. Cohen, L.L. Lodestro, and T.D. Rognlien for helpful comments. Work performed under the auspices of the U.S. DoE by UC LLNL under contract No W-7405-Eng-48.

References

1. P.A. Norreys, K.M. Krushelnick, and M. Zepf. Plasma Phys. Contr. Fus., **46**, B13-21 (2004)
2. S.J. Moon, S.C. Wilks, R.I. Klein, B.A. Remington, D.D. Ryutov, A.J. Mackinnon, P.K. Patel, A. Spitkovsky. Astrophys. Space Sci., **298**, 293, 2005.
3. L.O. Silva, R.A. Fonseca, J.W. Tonge, J.M. Dawson, W.B. Mori, M.V. Medvedev. Astrophysical Journal, Letters, **596**, L121, 2003.
4. M.S. Wei, F.N. Beg, E.L. Clark, A.E. Dangor, R.G. Evans, A. Gopal, K.W.D. Ledingham, P. McKenna, P.A. Norreys, M. Tatarakis, M. Zepf, K. Krushelnick. Phys. Rev. E **70**, 56412 (2004)
5. T. Katsouleas. Plasma Phys. Contr. Fus., **46**, B575-582 (2004)
6. R.A. Snavely, M.H. Key, S.P. Hatchett et al, Physical Review Letters, **85**, 2945, 2000
7. A.J. Mackinnon, M. Borghesi, S. Hatchett et al, Phys. Rev. Lett., **86**, 1769, 2001.
8. E. Liang. Astrophys. Space Sci., **298**, 211, 2005.
9. S.C. Wilks, H. Chen, E. Liang, P. Patel, D. Price, B. Remington, R. Shepherd, M. Tabak, W.L. Kruer. Astrophys. Space Sci., **298**, 347, 2005.
10. A. Pukhov, S. Gordienko, S. Kiselev, I. Kostyukov. Plasma Phys. Contr. Fus., **46**, B179 (2004).
11. S. Gordienko, A. Pukhov. Phys. Plasmas, **12**, 043109 (2005).
12. D.D. Ryutov, B.A. Remington. "Optimizing laboratory experiments for dynamic astrophysical phenomena." Paper presented at *3rd Intern. Conf. on Superstrong Fields in Plasmas*, Varenna, Sept. 19-24 2005 (To appear in AIP Proceedings, April 2006).
13. D.D. Ryutov, B.A. Remington. Plasma Phys. Contr. Fus., **48**, L23-L31, 2006.
14. T.M. Antonsen Jr, E. Ott. Appl. Phys. Lett, **28**, 424 (1976).
15. D.D. Ryutov, G.V. Stupakov. Fizika Plazmy, **2**, 767 (1976).
16. A.V. Arzhannikov, A.V, Burdakov, V.S. Koidan, D.D. Ryutov. ZHETF Letters, **24**, 19 (1976)
17. S. Humphries Jr. Nuclear Fusion, **20**, 1549 (1980).
18. M. Tatarakis, A. Gopal, I. Watts, F.N. Beg, A.E. Dangor, K. Krushelnick, U. Wagner, P.A. Norreys, Clark EL, Zepf M, Evans RG. Phys. Plasmas, **9**, 2244 (2002).
19. J.A. Stamper, Phys. Rev. Lett., **26**, 1012 (1971).
20. R. Sudan. Phys. Rev. Lett., **70**, 3075 (1993).
21. A.V. Gaponov, A. Miller. Soviet Physics JETP, **7**, 168 (1958).

Table 1. Switching to accelerating deuterium at an increased intensity

1	2	3	4	5	6	7	8	9	10	11
Quantity	Ion mass	Inten-sity	Fre-quency	Pulse du-ration	Spatial scale	Den-sity	Elec-tron energy	Ion energy	Quasi -static m.f.	Number of fast ions
Original system	M	I	ω	τ	L	n	W_e	W_i	B	N
"Primed" system	$2M$	$4I$	ω	τ	L	$2n$	$2W_e$	$2W_i$	$2B$	$2N$

The relative amplitude of the harmonics remains unchanged

Table 2. A scaled experiment at a reduced frequency

1	2	3	4	5	6	7	8	9	10
Quantity	Fre-quency	Inten-sity	Pulse du-ration	Spatial scale	Den-sity	Elec-tron energy	Ion energy	Quasi -static m.f.	Number of fast ions
Original system	ω	I	τ	L	n	W_e	W_i	B	N
"Primed" system	$\omega/2$	$I/4$	2τ	$2L$	$n/4$	W_e	W_i	$B/2$	$2N$

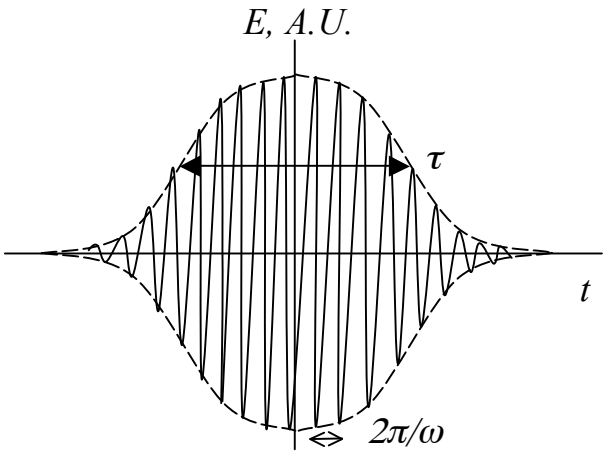

Fig 1. The temporal dependence of the electric field in an incident wave. The envelope function is of a form of $F(t/\tau)$, with τ being a characteristic width. In the scaling exercise, the function F must remain the same function of its argument, although the parameter τ may vary from system to system.

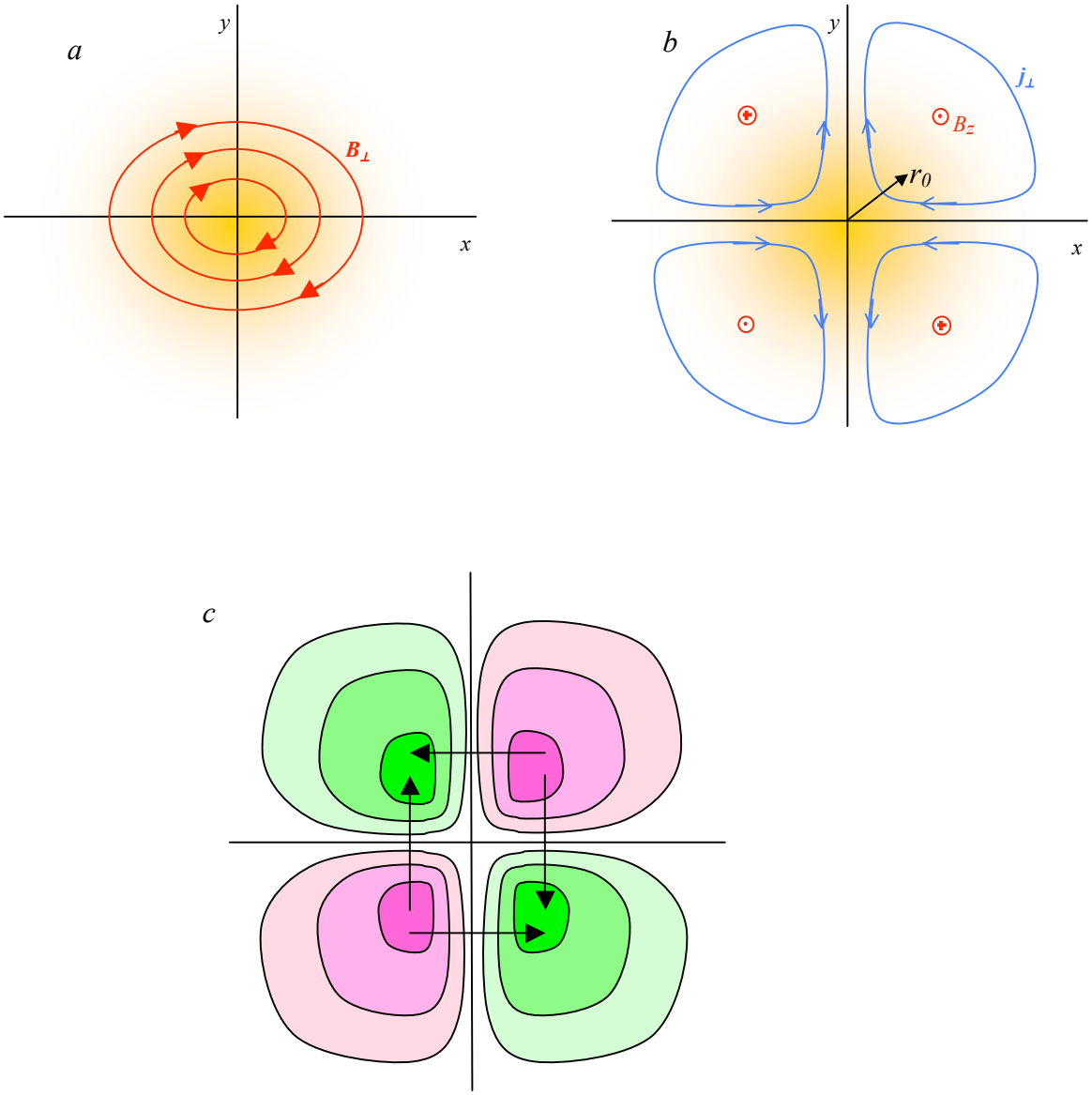

Fig. 2. Structure of the magnetic field generated by a laser beam at a normal incidence (a) Toroidal magnetic field; it is generated by the current that flows away from the viewer near the axis and toward the viewer at the periphery. (b) The current streamlines (arrows) generated in the case where the incident wave is linearly polarized, with the electric field being directed along the y axis. This current pattern leads to the generation of the poloidal magnetic field. (c) Distribution of the z-component of the magnetic field at some intermediate depth; The axial magnetic field lines are closed by a canopy of field lines near the ends of "solenoids". The direction of the closure is shown by arrows.

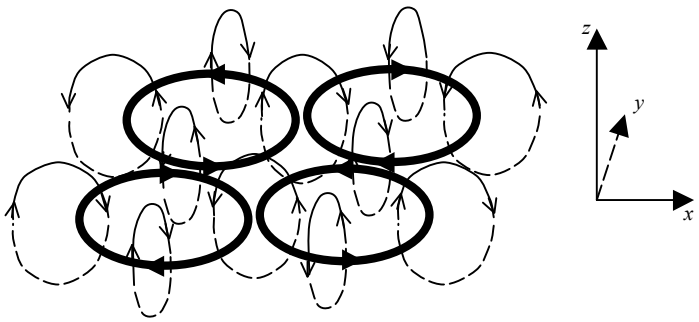

Fig. 3. A more detailed structure of the magnetic field in the case of a small axial extent of the current-carrying zone. The current loops are shown by thick lines. The magnetic field lines are shown in thin lines; dashed portions of these lines correspond to the zone beneath the plane where current loops are situated.